Assessment of the Passivation Capabilities of Two Different Covalent Chemical Modifications on GaP(100)

ARTICLE *in* LANGMUIR · JUNE 2010

Impact Factor: 4.46 · DOI: 10.1021/la904451x · Source: PubMed

3 AUTHORS, INCLUDING:

Dmitry Zemlyanov
Purdue University
132 PUBLICATIONS **1,802** CITATIONS
SEE PROFILE

Albena Ivanisevic
North Carolina State University
112 PUBLICATIONS **1,204** CITATIONS
SEE PROFILE

Langmuir
Article
pubs.acs.org/Langmuir

Assessment of the Passivation Capabilities of Two Different Covalent Chemical Modifications on GaP(100)

David Richards,[†] Dmitry Zemlyanov,[§] and Albena Ivanisevic*[,†,‡]

[†]*Weldon School of Biomedical Engineering,* [‡]*Department of Chemistry, and* [§]*Birck Nanotechnology Center, Purdue University, West Lafayette, Indiana 47906*

Received November 24, 2009. Revised Manuscript Received January 18, 2010

Gallium phosphide is a semiconductor material that can be used for the fabrication of optoelectronic devices. The report compares the ability of two similar organic molecules to form covalent bonds with the GaP(100) surface. Undecenoic acid (UDA) is a terminal alkene that can potentially form Ga−C bonds, and mercaptoundecanoic acid (MUA) is a thiol that can be used to generate Ga−S bonds. The chemical passivation capabilities of the functionalized surfaces exposed to different media were investigated by contact angle measurements, atomic force microscopy (AFM), and X-ray photoelectron spectroscopy (XPS). Toxicity levels, which are important for sensing applications, were evaluated by inductively coupled plasma mass spectrometry (ICP-MS) on the media in which surfaces were stored in order to identify any gallium leaching from the substrates. Both molecules formed fairly disordered monolayers demonstrated by comparable oxide thicknesses. The UDA molecules demonstrated better stability compared to MUA molecules based on contact angle measurements and tilt angle data extracted from XPS results. According to the XPS data, the UDA molecules formed a more dense adlayer compared to MUA molecules. With respect to toxicity, the UDA-functionalized GaP provided better passivation which was confirmed by less gallium leaching into water and saline solutions. Overall, the superior passivation provided by UDA demonstrates that alkene grafting has better potential for modifying GaP based devices such as implantable sensors.

Introduction

The ability to manipulate inorganic surfaces with organic molecules can result in the advancement of many scientific fields including chemistry, electrical engineering, medicine, and biology.[1] More specifically, the adsorption of organic molecules onto a semiconductor surface has the potential to make biosensors more biocompatible and allow them to be implantable.[2−4] Silicon has been a heavily researched semiconductor surface for chemical passivation due mainly to its domination of the optoelectronic industry. Common strategies for silicon functionalization include silanization and polymer grafting. Alkene grafting has also been investigated and has demonstrated promising results in terms of stability and monolayer formation on silicon surfaces.[5,6] Recently, functionalization of semiconductor surfaces has been extended to III−V materials whose superior optoelectronic properties make them ideal for sensing applications. The goal is to combine these favorable properties with a tailored surface to render the substrate biocompatible and selectively reactive. Due to its promising characteristics for device fabrication, gallium arsenide (GaAs) has been extensively studied and the formation of self-assembled monolayers has been of interest.[7−12] Relatively few reports extend functionalization to other III−V materials.

Thiols such as octadecanethiol,[12] hexadecanethiol,[11] and mercaptohexadecanoic acid,[8] among others, have been adsorbed onto a GaAs surface with the result of increasing the photoluminescence (PL). PL is a common method for quantifying the reduction of surface states caused by dangling surface bonds and a native oxide layer, making it an appropriate assessment of passivation. Grafting with a conjugated molecule to GaAs has also been demonstrated, resulting in a highly stable monolayer due to the formation of strong Ga−C and As−C bonds.[13] To a lesser extent, alkanethiol adsorption has been reported on GaN,[14] GaP,[15,16] InAs,[17] and InP.[16,18] Photochemical grafting to GaP[19] and GaN[20] has also been performed, again showing good stability. Gallium phosphide (GaP) is a III−V semiconductor with an indirect band gap that is commonly used in light-emitting

*To whom correspondence should be addressed. E-mail: albena@purdue.edu.

(1) Swalen, J. D.; Allara, D. L.; Andrade, J. D.; Chandross, E. A.; Garoff, S.; Israelachvili, J.; McCarthy, T. J.; Murray, R.; Pease, R. F.; Rabolt, J. F.; Wynne, K. J.; Yu, H. *Langmuir* **1987**, *3*, 932–950.
(2) Fritz, J.; Cooper, E. B.; Gaudet, S.; Sorger, P. K.; Manalis, S. R. *Proc. Natl. Acad. Sci. U.S.A.* **2002**, *99*, 14142–14146.
(3) Lee, M.; Fauchet, P. M. *Opt. Express* **2007**, *15*, 4530–4535.
(4) Uslu, F.; Ingebrandt, S.; Mayer, D.; Bocker-Meffert, S.; Odenthal, M.; Offenhausser, A. *Biosens. Bioelectron.* **2004**, *19*, 1723–1731.
(5) Buriak, J. M. *Chem. Rev.* **2002**, *102*, 1271–1308.
(6) Linford, M. R.; Fenter, P.; Eisenberger, P. M.; Chidsey, C. E. D. *J. Am. Chem. Soc.* **1995**, *117*, 3145–3155.
(7) Ding, X.; Moumanis, K.; Dubowski, J. J.; Frost, E. H.; Escher, E. *Appl. Phys. A: Mater. Sci. Process.* **2006**, *83*, 357–360.
(8) Ding, X. M.; Moumanis, K.; Dubowski, J. J.; Tay, L.; Rowell, N. L. *J. Appl. Phys.* **2006**, *99*, 054701.
(9) Lunt, S. R.; Ryba, G. N.; Santangelo, P. G.; Lewis, N. S. *J. Appl. Phys.* **1991**, *70*, 7449–7465.
(10) Lunt, S. R.; Santangelo, P. G.; Lewis, N. S. *J. Vac. Sci. Technol., B* **1991**, *9*, 2333–2336.
(11) Moumanis, K.; Ding, X.; Dubowski, J. J.; Frost, E. H. *J. Appl. Phys.* **2006**, *100*, 034702.
(12) Nakagawa, O. S.; Ashok, S.; Sheen, C. W.; Martensson, J.; Allara, D. L. *Jpn. J. Appl. Phys. 1* **1991**, *30*, 3759–3762.
(13) Stewart, M. P.; Maya, F.; Kosynkin, D. V.; Dirk, S. M.; Stapleton, J. J.; McGuiness, C. L.; Allara, D. L.; Tour, J. M. *J. Am. Chem. Soc.* **2004**, *126*, 370–378.
(14) Bermudez, V. M. *Langmuir* **2003**, *19*, 6813–6819.
(15) Flores-Perez, R.; Zernlyanov, D. Y.; Ivanisevic, A. *J. Phys. Chem. C* **2008**, *112*, 2147–2155.
(16) Zerulla, D.; Chasse, T. *J. Electron. Spectrosc.* **2009**, *172*, 78–87.
(17) Tanzer, T. A.; Bohn, P. W.; Roshchin, I. V.; Greene, L. H.; Klem, J. F. *Appl. Phys. Lett.* **1999**, *75*, 2794–2796.
(18) Schvartzman, M.; Sidorov, V.; Ritter, D.; Paz, Y. *J. Vac. Sci. Technol., B* **2003**, *21*, 148–155.
(19) Flores-Perez, R.; Zemlyanov, D. Y.; Ivanisevic, A. *ChemPhysChem* **2008**, *9*, 1528–1530.
(20) Kim, H.; Colavita, P. E.; Metz, K. M.; Nichols, B. M.; Sun, B.; Uhlrich, J.; Wang, X. Y.; Kuech, T. F.; Hamers, R. J. *Langmuir* **2006**, *22*, 8121–8126.

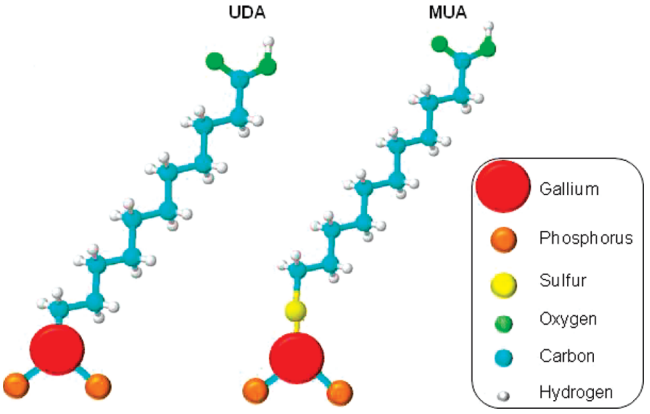

Figure 1. Schematic representations of the covalent attachments to the surface.

and high temperatures devices. Like all III−V semiconductor materials, it quickly forms an unstable oxide layer leading to difficulties in procedures that involve aqueous solutions. Such oxide layers can dissolve from the surface which causes problems with respect to stability and can lead to increased levels of Ga which can be toxic. A few studies have reported on the passivation of GaP with sulfides to prevent oxide formation,[21,22] and previously we reported on passivation with thiols containing chemically reactive groups.[15]

In this study, we compare the chemical modification of GaP(100) with two similar organic molecules, one containing a thiol and one with a terminal alkene. This allows us to investigate the different passivation capabilities of two different covalent attachments to the surface. The adsorbates we used were 11-mercaptoundecanoic acid (MUA) and undecenoic acid (UDA). MUA is a thiol that is capable of forming a Ga−S covalent bond, while UDA is a terminal alkene capable of forming a Ga−C covalent bond upon exposure to UV light (Figure 1). It has been shown that covalent attachment to the phosphorus atom does not readily occur.[16] Photochemical grafting is a faster and cleaner process compared to thiol adsorption. The conditions required for grafting are less hazardous (no high temperatures or high vacuum) and less time-consuming due to the alkene's ability to form covalent bonds with the surface by way of a radical initiation step caused by irradiation with UV light.[6]

Various surface sensitive characterization techniques were used to evaluate the functionalized surfaces including water contact angle measurement, X-ray photoelectron spectroscopy (XPS), and atomic force microscopy (AFM). Functionalized surfaces were exposed to water and various pH solutions to investigate stability, and saline with varying concentrations of H_2O_2 to simulate oxidative physiological conditions.[23] In order to evaluate the toxicity, inductively coupled plasma mass spectrometry (ICP-MS) was performed on the various solutions that were exposed to the functionalized substrates to determine the amount of gallium leaching from the functionalized surfaces.

Experimental Section

Surface Cleaning and Modification. Wafers of S-doped GaP(100) were purchased from University Wafer (South Boston, MA). Undecenoic acid (UDA, 98%) and a 5 mM ethanolic solution of 11-mercaptoundecanoic acid (MUA) were purchased from Sigma-Aldrich. The GaP wafers were cut into 1×1 cm^2 pieces. Pieces designated for UDA functionalization were ultrasonically degreased with water and ethanol and subsequently dried with N_2. The cleaned samples were immersed in NH_4OH, rinsed with water, and dried with N_2. The samples were exposed to a 10% solution of UDA in toluene for 3 h under a N_2 atmosphere. All samples were rinsed with ethanol and dried with N_2 before characterization.

The samples designated for MUA functionalization were ultrasonically degreased with water, ethanol, and methanol and subsequently dried with N_2. The samples were then exposed to aqua regia solution (HCl (36%)/HNO_3 (70%), 3:1/v:v) for 30 s at 40 °C. The samples were rinsed with water and dried with N_2. The cleaned samples were exposed to a 1 mM ethanolic solution of MUA for 24 h. All samples were then rinsed with ethanol and dried with N_2.

Stability Experiments. Solutions (1 mL) of water as well as buffer solutions of pH 5, 7, and 9, saline, and saline with 0.1%, 1%, and 10% H_2O_2 were created and placed in 1 mL plastic vials. One UDA-functionalized GaP sample was placed in each vial. The samples were removed from the vials and washed with ethanol and dried with N_2 after their respective time period of 1, 5, or 7 days. The samples were immediately subjected to contact angle measurements and then placed in an inert atmosphere until they were analyzed by XPS. The process was repeated for MUA-functionalized surfaces. All solutions were kept in the plastic vial until they were ready for ICP-MS.

Surface Characterization. Water contact angle measurements were performed on a Tantac, Inc. contact angle meter, model CAM-PLUS, using the half angle method. At least five readings were taken on each sample and averaged.

AFM images were collected using the tapping mode setting on a Multi-Mode Nanoscope IIIa atomic force microscope. A scan size of 1×1 μm^2 at a rate of 2 Hz was used on each sample. Single beam cantilevers were purchased from Veeco Instruments. Data analysis was performed using the Nanoscope III 5.12r3 software.

XPS data were obtained with a Kratos Ultra DLD spectrometer using monochromatic Al Kα radiation ($h\nu$ = 1486.58 eV). Survey and high resolution spectra were collected at a fixed analyzer pass energy of 160 and 20 eV, respectively, and acquisition was performed at photoemission angles of 0° and 60° measured with respect to the surface normal. Binding energy values were referenced to the Fermi edge, and charge correction was done using the C 1s peak set at 284.80 eV. Curve fitting was performed after linear or Shirley type background subtraction assuming a Gaussian/Lorentzian peak shape.

ICP-MS data were obtained with an Element2 ICP mass spectrometer (ThermoFisher, Bremen, Germany) equipped with an Aridus desolvating introduction system (with a T1H nebulizer) to enhance sensitivity and reduce oxide and hydride interferences (Cetac Technologies, Omaha, NE). The argon sweep gas and nitrogen of the Aridus were adjusted for maximum peak height and stability using 7Li, 115In, and 238U peaks obtained from a Merck multielement standard (1 ng/mL, Merck & Co.). After tuning and calibration of the ICP instrument, medium resolution analyses were carried out on the Ga69 and Ga71 peaks.

Results and Discussion

Initial Surface Characterization. Prior to functionalization with the organic molecules, the contact angle of the bare GaP substrate was 0°, or total wetting, indicating a clean hydrophilic surface. After incubation in the respective organic molecule, the contact angle increased. Functionalization with UDA increased the contact angle to 77 ± 5°, while MUA functionalization increased the contact angle to 64 ± 5°. This increased contact angle can be attributed to the surface not being terminated with the hydrophilic carboxylic acid groups, but rather the hydrophobic carbon backbone of the molecules lying flat on the surface.

(21) Liu, K. Z.; Suzuki, Y.; Fukuda, Y. *Surf. Interface Anal.* **2004**, *36*, 966–968.
(22) Suzuki, Y.; Sanada, N.; Shimomura, A.; Fukuda, Y. *Appl. Surf. Sci.* **2004**, *235*, 260–266.
(23) Metz, K. M.; Mangham, A. N.; Bierman, M. J.; Jin, S.; Hamers, R. J.; Pedersen, J. A. *Environ. Sci. Technol.* **2009**, *43*, 1598–1604.

Table 1. Summary of Surface Roughness of Clean GaP and GaP Functionalized with UDA and MUA

surface	roughness (nm)
clean GaP	0.17 ± 0.02
UDA-functionalized GaP	0.32 ± 0.09
MUA-functionalized GaP	0.28 ± 0.03

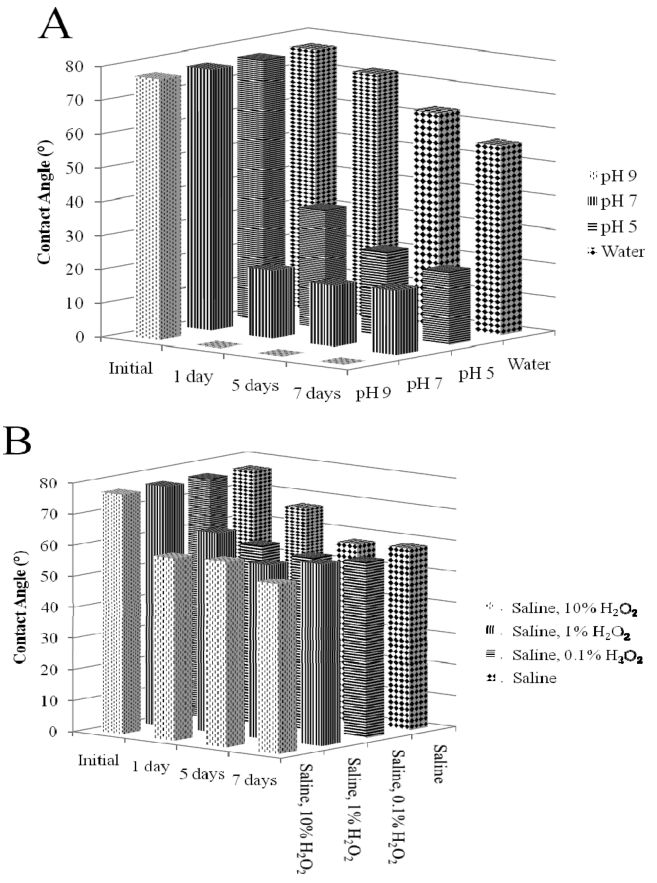

Figure 2. Average contact angle measurements of UDA-functionalized surface for (A) water and various pH solutions and (B) varying concentrations of H_2O_2 in saline. (Error of $\pm 5°$ for each measurement.)

Further characterization of the surface was done with AFM prior to exposing the samples to any solutions. AFM scans of the surface revealed information about the surface roughness. Average roughness values can be found in Table 1. A clean GaP surface had a roughness of about 0.17 nm. This value was used as a reference for the functionalized surfaces. The roughness values of the functionalized surfaces were comparable. The UDA surface seemed to have a slightly higher roughness than the MUA surface. The slight increase in roughness of the surfaces with respect to the reference indicates that a homogeneous layer of adsorbed molecules is present, and no evidence of clustering of adsorbates was found.

Contact Angle Characterization after Solution Exposure. Contact angle measurements were performed on all samples immediately after removing them from their designated solutions and washing. A summary of the results can be found in Figures 2 and 3. Exposing UDA-terminated surfaces to water resulted in a steady decrease in contact angle down to a value of $56 \pm 5°$ at 7 days. Exposure to pH 5 also resulted in a steady decrease with a 7 day contact angle measurement of $22 \pm 5°$; however, pH 7 samples show a steady value of roughly 19° throughout each time

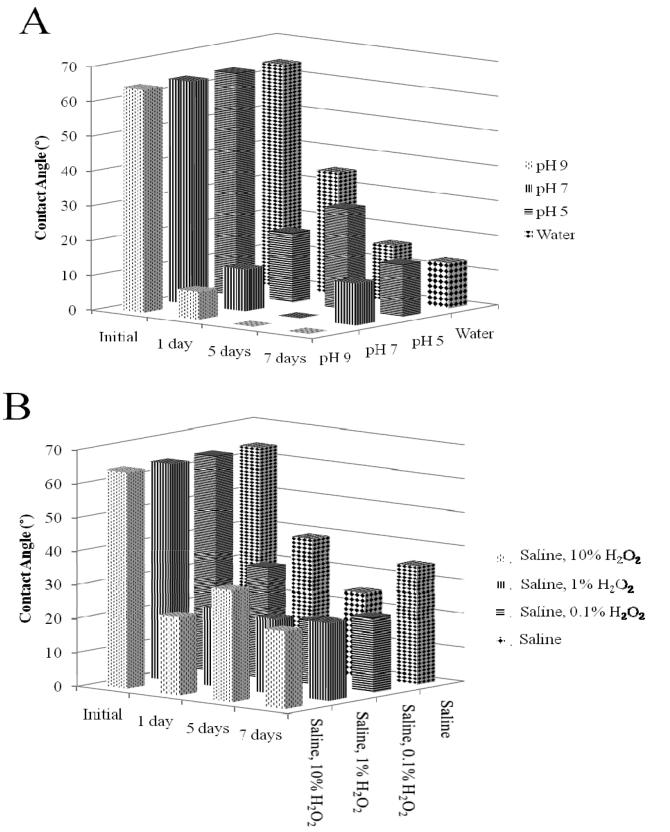

Figure 3. Average contact angle measurements of MUA-functionalized surface for (A) water and various pH solutions and (B) varying concentrations of H_2O_2 in saline. (Error of $\pm 5°$ for each measurement.)

period. Samples immersed in a pH 9 solution showed total wetting after the first day and throughout until 7 days. The decreased stability of alkene grafting on III−V semiconductors in basic conditions has been demonstrated in other reports.[24] The UDA-functionalized surfaces that were exposed to different concentrations of H_2O_2 in saline showed a different trend. These samples level out to a roughly constant value of 58° after the first day, indicating that H_2O_2 has a negligible effect on the stability of the monolayer. MUA-functionalized samples exposed to the various solutions showed similar trends. Again, a steady decrease was seen when samples were exposed to water. Solutions of pH 5 showed the highest contact angles compared to the other pH solutions, while samples exposed to pH 9 demonstrated total wetting after 5 days. Within experimental error, the samples immersed in various saline/H_2O_2 solutions showed a general leveling off after the first day. The significantly large decrease in contact angle compared to the samples immersed in water (pH $\sim$ 8) is attributed to the harsh nature of the chemicals in the buffer solution. These chemicals effectively etch the surface, breaking the Ga−C and Ga−S bonds while also removing the native oxide layer. This is further confirmed by XPS and ICP-MS data (see below).

X-ray Photoelectron Spectroscopy. XPS has the ability to provide both quantitative and qualitative information about the clean and modified surfaces. We obtained high resolution XPS spectra of C 1s, O 1s, Ga 3d, Ga 2p, and P 2p core levels from each of the samples after exposure to their respective solutions. Since the binding energy of the S 2p core level overlaps with the binding energy of the Ga 3s, S 2s, and S 2p core levels, spectra were taken

(24) Kim, H.; Colavita, P. E.; Paoprasert, P.; Gopalan, P.; Kuech, T. F.; Hamers, R. J. *Surf. Sci.* **2008**, *602*, 2382–2388.

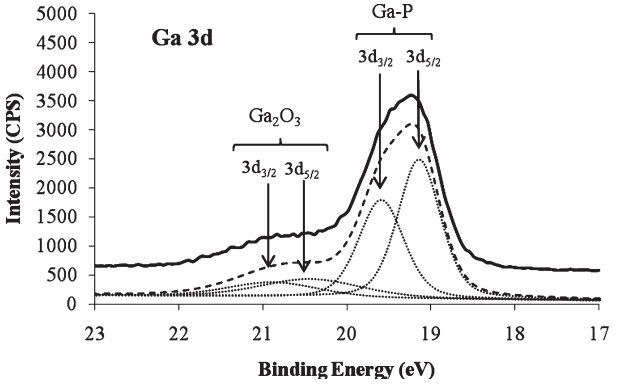

Figure 4. High resoulution XPS spectrum of the Ga 3d region collected from a sample functionalized with UDA and stored in water for 1 day. The collected spectrum is shown in a solid line, and all deconvolutions are in dashed lines.

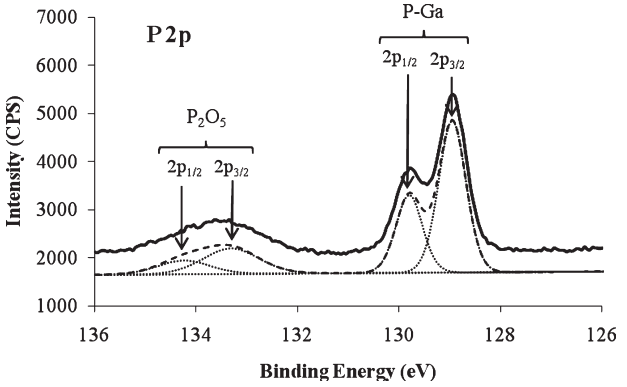

Figure 5. High resolution XPS spectrum of the P 2p region collected from a sample functionalized with UDA and stored in saline for 7 days. The collected spectrum is shown in a solid line, and all deconvolutions are in dashed lines.

from each of the MUA-functionalized surfaces. In addition, a clean GaP sample and a functionalized control sample were analyzed by XPS as references. For each sample, the XPS data were collected at a photoelectron emission angle of 0° and 60°.

Figure 4 depicts a representative Ga 3d high resolution spectrum. Two chemical states of gallium can be detected. A spin−orbital splitting doublet with the Ga $3d_{5/2}$ peak at 19.2 eV corresponds to gallium bound to phosphorus, while the doublet with the Ga $3d_{5/2}$ peak at 20.6 eV is representative of the oxide Ga_2O_3. The peaks corresponding to gallium bound to sulfur or carbon could not be resolved. Figure 5 is a representative P 2p high resolution spectrum. A spin−orbital doublet with the P $2p_{5/2}$ peak at 129 eV corresponds to phosphorus bound to gallium, while the doublet with the P $2p_{5/2}$ peak around 133.5 eV is the phosphorus oxide, P_2O_5.

Collecting XPS spectra at different photoemission angles allows us to calculate the thickness of the oxide layer. The oxide layer thickness was calculated using the Ga 3d spectra and an approach adapted from Fadley.[25] Assuming a semi-infinite substrate with oxide overlayer thickness t, we can write eqs 1 and 2 for the peak intensities of the substrate and oxide overlayer, respectively:

$$N_{GaP}(\theta) = C_{inst}\rho_{GaP}\frac{d\sigma_s}{d\Omega}\Lambda_e^{GaP}(E_{Ga3d}) \cos\theta \exp\left(\frac{-t}{\Lambda_e^{Ga_2O_3}(E_{Ga3d})\cos\theta}\right) \quad (1)$$

$$N_{Ga_2O_3}(\theta) = C_{inst}\rho_{Ga_2O_3}\frac{d\sigma_l}{d\Omega}\Lambda_e^{Ga_2O_3}(E_{Ga3d}) \cos\theta\left(1 - \exp\left(\frac{-t}{\Lambda_e^{Ga_2O_3}(E_{Ga3d})\cos\theta}\right)\right) \quad (2)$$

where N_{GaP} and $N_{Ga_2O_3}$ are the peak intensities from the substrate and oxide overlayer, respectively. C_{inst} is a constant associated with the spectrometer (this includes X-ray intensity, detection efficiency, collection angle, etc.), ρ_{GaP} and $\rho_{Ga_2O_3}$ are the density of gallium atoms in the gallium phosphide substrate and gallium oxide overlayer, respectively, measured in atoms/cm^3; $d\sigma_k/d\Omega$ and $d\sigma_l/d\Omega$ are differential cross sections, which can be calculated

(25) Fadley, C. S. *Basic Concepts of X-ray Photoelectron Spectroscopy*; Pergamon Press: New York, 1978; Vol. *11*, Chapter 1.

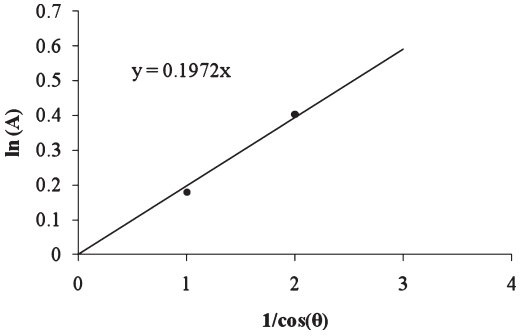

Figure 6. Representative graph used to determine oxide thickness for a sample functionalized with UDA prior to any solution exposure. The y-axis, represented as ln(A), is the left-hand side of eq 4.

using tabulated Scofield cross sections and the Reilman asymmetric parameters, $\Lambda_e^{GaP}(E_{Ga3d})$ and $\Lambda_e^{Ga_2}O_3(E_{Ga3d})$ are electron attenuation lengths of the substrate and gallium oxide overlayer, respectively, and θ is the photoemission angle. Taking the ratio of the overlayer and substrate peak intensities, we obtain eq 3:

$$\frac{N_{Ga_2O_3}(\theta)}{N_{GaP}(\theta)} = \frac{\rho_{Ga_2O_3}\Lambda_e^{Ga_2O_3}(E_{Ga3d})\left[1 - \exp\left(\frac{-t}{\Lambda_e^{Ga_2O_3}(E_{Ga3d})\cos\theta}\right)\right]}{\rho_{GaP}\Lambda_e^{GaP}(E_{Ga3d})\exp\left(\frac{-t}{\Lambda_e^{Ga_2O_3}(E_{Ga3d})\cos\theta}\right)} \quad (3)$$

This equation can be simplified to the following expression (eq 4):

$$\ln\left(\frac{N_{GaP}(\theta)}{N_{Ga_2O_3}(\theta)}\frac{\rho_{Ga_2O_3}}{\rho_{GaP}}\frac{\Lambda_e^{Ga_2O_3}(E_{Ga3d})}{\Lambda_e^{GaP}(E_{Ga3d})} + 1\right) = \frac{t}{\Lambda_e^{GaP}(E_{Ga3d})}\frac{1}{\cos\theta} \quad (4)$$

The oxide layer is finally calculated with a least-squares fit of $1/\cos(\theta)$ versus $\ln\{[N_{GaP}(\theta)/N_{Ga_2O_3}(\theta)][\rho_{Ga_2O_3}/\rho_{GaP}][\Lambda_e^{Ga_2}O_3(E_{Ga3d})/\Lambda_e^{GaP}(E_{Ga3d})] + 1\}$ to obtain $t/\Lambda_e^{GaP}(E_{Ga3d})$. Figure 6 depicts a representative graph used to obtain the oxide thickness.

One can multiply the slope by the attenuation length for Ga 3d photoelectrons and obtain the desired oxide layer thickness. Attenuation length can be calculated using NIST SRD-82 software. A summary of the calculated oxide thicknesses for each

Table 2. Summary of Oxide Thickness and Ga/P Peak Intensity Ratio Calculated by XPS (Error Range Was Calculated Using the Standard Deviation of the Least Squares Fit)

		oxide thickness (Å)		Ga/P	
	sample	UDA-functionalized	MUA-functionalized	UDA-functionalized	MUA-functionalized
water	clean	3 ± 1	4 ± 1	1.18	0.99
	control	3 ± 1	4 ± 1	1.20	1.27
	1 day	8 ± 4	4 ± 2	1.31	1.30
	5 days	11 ± 5	17 ± 9	1.63	1.38
	7 days	14 ± 7	8 ± 4	1.59	1.37
pH 5	1 day	2 ± 1	4 ± 2	1.27	1.23
	5 days	3 ± 2	4 ± 2	1.18	1.26
	7 days	2 ± 2	4 ± 2	1.30	1.30
pH 7	1 day	2 ± 1	4 ± 2	1.23	1.33
	5 days	2 ± 2	4 ± 2	1.17	1.25
	7 days	3 ± 2	4 ± 2	1.35	1.30
pH 9	1 day	2 ± 2	4 ± 2	1.20	1.29
	5 days	2 ± 2	4 ± 2	1.29	1.17
	7 days	3 ± 1	4 ± 2	1.33	1.32
saline	1 day	7 ± 4	4 ± 2	1.29	1.19
	5 days	12 ± 6	5 ± 3	1.38	1.27
	7 days	10 ± 5	7 ± 4	1.56	1.35
saline, 0.1% H_2O_2	1 day	14 ± 2	9 ± 4	1.54	1.29
	5 days	11 ± 3	14 ± 7	1.41	1.44
	7 days	12 ± 2	17 ± 8	1.49	1.49
saline, 1% H_2O_2	1 day	15 ± 8	12 ± 6	1.49	1.31
	5 days	15 ± 8	15 ± 7	1.44	1.47
	7 days	15 ± 8	18 ± 9	1.42	1.48
saline, 10% H_2O_2	1 day	13 ± 6	11 ± 5	1.33	1.35
	5 days	17 ± 8	20 ± 10	1.44	1.41
	7 days	10 ± 5	15 ± 8	1.42	1.42

solution is found in Table 2. Within experimental error, the values are relatively similar for each functionalization. This similarity suggests that each modification resulted in a sparsely packed monolayer resulting in many voids between each organic molecule. These voids gave rise to the oxide layer demonstrated by the XPS data. This low coverage can be explained by the relatively small length of the molecules (11-carbon) coupled with the large hydrophilic carboxylic acid group that presents steric hindrance which prevents the formation of a dense monolayer.[8] The lowest oxide thickness values are seen in the various pH buffer solutions which again supports the finding that the composition of the buffer (described earlier) etches any oxide layer after it forms.

Table 2 also summarizes the ratio of Ga and P calculated based on Ga 3d and P 2p peak intensities. This information was used to identify any gallium enrichment of the surface. A general increase in the Ga/P ratio can be seen in the surfaces exposed to solutions compared to the clean surface which is attributed to the greater solubility of the phosphorus oxide (P_2O_5) compared to the gallium oxide (Ga_2O_3).[26,27] In each functionalization, there is a decreased Ga/P ratio associated with the pH buffer solutions compared to the other solutions, indicating greater solubility of Ga_2O_3 in the buffer conditions.

XPS data were also used to calculate the adlayer thickness using the equation

$$N_{\mathrm{Ga3d(P2p)}} = N^0_{\mathrm{Ga3d(P2p)}}\left(1 - \frac{-t}{e^{\Lambda_{\mathrm{Ga3d(P2p)}}\cos(\theta)}}\right) \qquad (5)$$

(26) Lide, D. R.; *CRC handbook of chemistry and physics*; CRC Press: Cleveland, OH, 1977.
(27) Ghidaoui, D.; Lyon, S. B.; Thompson, G. E.; Walton, J. *Corros. Sci.* **2002**, *44*, 501–509.

Table 3. Adlayer Thickness and Tilt Angle for UDA and MUA Functionalized GaP

surface functionalization	calculated thickness with Ga 3d (Å)	calculated thickness with P 2p (Å)	length of molecule (Å)	average tilt angle from surface normal (°)
UDA	9 ± 2	8 ± 2	14.80	55 ± 10
MUA	1 ± 2	2 ± 2	15.42	84 ± 7

$N_{\mathrm{Ga3d\ (P2p)}}$ and $N^0_{\mathrm{Ga3d\ (P2p)}}$ are peak intensities of Ga 3d and P 2p before and after functionalization, respectively. $\Lambda_{\mathrm{Ga3d\ (P2p)}}$ is the electron attenuation length of Ga 3d or P 2p photoelectrons through the UDA and MUA adlayers, θ is the photoemission angle, and t is the thickness of the adlayer in Å. Values for electron attenuation length were obtained using the NIST SRD-82 software. The adlayer thickness was calculated using both the Ga 3d and P 2p spectra which can be found in Table 3. The thickness calculation of the UDA adlayer resulted in a value of 9 ± 2 Å from the Ga 3d spectrum and 8 ± 2 Å from the P 2p spectrum. The thickness of the MUA adlayer was 1 ± 2 Å from the Ga 3d spectrum and 2 ± 2 Å from the P 2p spectrum. Using the values for the adlayer thickness, we were able to calculate the mean tilt angle after each functionalization. We estimate a tilt angle of roughly 55 ± 10° for UDA and 84 ± 7° for MUA assuming the molecular lengths were 14.80 and 15.42 Å, respectively. The tilt angle calculations suggest that the MUA forms a more disordered monolayer on the GaP surface compared to UDA.

Finally, the XPS data were used to calculate the coverage of each of the molecules on the GaP surface using the following equation:

$$\text{coverage} \equiv \frac{s_{\mathrm{adlayer}}}{s_{\mathrm{substrate}}} = \frac{N_{\mathrm{adlayer}}(\theta)}{N_{\mathrm{GaP}}(\theta)} \frac{\frac{d\sigma_k}{d\Omega}\Lambda_e^{\mathrm{GaP}}(E_s)\cos\theta}{\frac{d\sigma_l}{d\Omega}d} \qquad (6)$$

where $N_{\mathrm{adlayer}}(\theta)$ and $N_{\mathrm{GaP}}(\theta)$ are the peak intensities of the adlayer and Ga 3d or P 2p, respectively; $d\sigma_k/d\Omega$ and $d\sigma_l/d\Omega$ are differential cross sections, $\Lambda_e^{\mathrm{GaP}}(E_s)$ is the Ga 3d or P 2p electron attenuation length, d is the distance between adjacent gallium (phosphorus) planes for GaP(100), and θ is the electron emission angle. The coverage in monolayers (ML, the ratio between the number of adsorbed molecules and surface atoms of the substrate) was calculated using both the Ga 3d and P 2p spectra at 0° and 60° and can be found in Table 4. To account for interference from atmospheric hydrocarbon contamination, curve-fitting of the C 1s peak was employed and the C 1s component corresponding to the carboxyl atom (HO—C═O) was used to extract the exact amount of UDA or MUA that was actually present on the surface. The actual amount of UDA or MUA present on the surface was used in eq 6 to obtain the coverage. The coverage values suggest that the UDA formed approximately a monolayer, whereas the MUA-functionalized surface covered up to half of a monolayer. This again indicates better passivation of UDA compared to MUA.

Inductively Coupled Plasma Mass Spectrometry (ICP-MS). Inductively coupled plasma mass spectrometry (ICP-MS) was performed on each of the "7 day" solutions for each functionalization to investigate the amount of gallium leaching from the sample surfaces and to assess toxicity levels after prolonged exposure. The concentration of gallium in the water solution exposed to a MUA-functionalized surface was over 5 times higher than that in the water solution exposed to a UDA-functionalized surface. With respect to the saline solution, the gallium concentration was over 7 times higher for the MUA-functionalized

Table 4. Coverage in Monolayers (ML) for UDA and MUA Functionalized GaP

	coverage (ML)			
	UDA-functionalized		MUA-functionalized	
angle	Ga 3d	P 2p	Ga 3d	P 2p
0°	1.0	1.2	0.3	0.4
60°	1.3	1.5	0.4	0.5

Table 5. Gallium Concentration in Water and Saline "7 day" Solutions after Exposure to UDA and MUA-Functionalized Surfaces

	gallium concentration (ppb)	
sample solution	UDA-functionalized	MUA-functionalized
water, 7 days	300 ± 90	1600 ± 500
saline, 7 days	60 ± 20	450 ± 130

surface (Table 5). More covalent attachments from the organic molecules to the GaP surface results in less bonds being available for the formation of an oxide (Ga_2O_3) that has the potential to dissolve and become present in the surrounding media. These data further support the notion that the UDA forms a more ordered monolayer capable of passivating the GaP surface more efficiently. It is important to note that passivation by thiol monolayers on GaAs has shown to be ineffective in a previous study.[28]

The effects of elevated gallium levels in humans and mice have been studied previously. Researchers have identified that gallium accumulation occurs primarily in the kidney.[29] In a study that focused on the antitumor properties of gallium in humans, prolonged retention of blood plasma levels of 1.9 ppm resulted in minimal damage to the kidney.[30] Elevated gallium levels also showed favorable results when compared to other group III elements such as aluminum, indium, and thallium, which was evidenced by decreased mortality in mice and rats upon gallium nitrate injection.[31] For comparison, the amount of gallium present in normal river water, drinking water, and urine is on the order of ~1 ppb.[32,33]

ICP-MS data from the various pH solutions are shown in Table 6. The data indicate a large amount of gallium leaching into the buffer solutions. As mentioned previously, this is attributed to the harsh nature of the chemicals used in the buffer. Within error, the gallium concentration values remain relatively consistent throughout each different pH solution, indicating that the effects of the acidic or basic conditions are overwhelmed by the buffer chemicals. Moreover, neither functionalization provides better

Table 6. Gallium Concentration in pH Buffer Solutions after Exposure to UDA and MUA-Functionalized Surfaces

	gallium concentration (ppm)	
sample solution	UDA-functionalized	MUA-functionalized
pH 5, 7 days	4.7 ± 1.5	3.8 ± 1.5
pH 7, 7 days	5.1 ± 1.5	5.3 ± 2.0
pH 9, 7 days	5.1 ± 1.5	3.5 ± 2.0

Table 7. Gallium Concentration in Saline/H_2O_2 Solutions after Exposure to UDA and MUA-Functionalized Surfaces

	gallium concentration (ppb)	
sample solution	UDA-functionalized	MUA-functionalized
saline 0.1% H_2O_2, 7 days	70 ± 20	50 ± 20
saline 1% H_2O_2, 7 days	160 ± 50	120 ± 40
saline 10% H_2O_2, 7 days	80 ± 30	80 ± 30

passivation, within error, which can further be attributed to the harsh buffer chemicals. These chemicals quickly etch away at the chemisorbed molecules and begin dissolving the underlying gallium. This process seems to occur at a similar rate in each functionalization.

Table 7 summarizes the gallium concentration of the various saline/H_2O_2 solutions. Macrophages are known to release H_2O_2, and so this mixture attempts to mimic physiological conditions.[34] Within error, the data suggest that H_2O_2 has little effect on the amount of gallium leached into the surrounding media from both functionalizations. Also, the gallium leaching seems to not depend on the functionalization. This finding can be explained by the oxidizing nature of H_2O_2 that forms soluble Ga_2O_3 at exposed GaP sites at an equal rate.

Conclusions

This study assesses the passivation capabilities of two similar organic molecules with different covalent attachments to a GaP surface. Contact angle measurements provide initial insight into the stability of the adlayers. AFM data provided evidence for a smooth adlayer. XPS data indicate that neither functionalization has an advantage over the other with respect to reducing the amount of oxide formation, suggesting that the voids between molecules are large. However, XPS was able to indicate a more dense adlayer of UDA compared to MUA evidenced by adlayer coverage and tilt angle data. Finally, toxicity was assessed using ICP-MS which indicated that less gallium was leached into the surrounding media when the surface was functionalized with UDA. A terminal alkene grafting procedure seems to be more stable and better suited for passivation of a GaP(100) surfaces that might be considered as part of implantable devices.

Acknowledgment. This work was supported by NSF under CHE-0614132. We thank Arlene Rothwell and Dr. Karl Wood for help with ICP-MS measurements.

(28) Kirchner, C.; George, M.; Stein, B.; Parak, W. J.; Gaub, H. E.; Seitz, M. *Adv. Funct. Mater.* **2002**, *12*, 266–276.
(29) Nakamura, K.; Fujimori, M.; Tsuchiya, H.; Orii, H. *Anal. Chim. Acta* **1982**, *138*, 129–136.
(30) Kelsen, D. P.; Alcock, N.; Yeh, S.; Brown, J.; Young, C. *Cancer* **1980**, *46*, 2009–2013.
(31) Hart, M. M.; Adamson, R. H. *Proc. Natl. Acad. Sci. U.S.A.* **1971**, *68*, 1623–.
(32) Antheraidis, A. N.; Zachariadis, G. A.; Stratis, J. A. *Talanta* **2003**, *60*, 929–936.
(33) Pozo, M. E. U.; Detorres, A. G.; Pavon, J. M. C. *Anal. Chem.* **1987**, *59*, 1129–1133.
(34) Linsmeier, C. E.; Wallman, L.; Faxius, L.; Schouenborg, J.; Bjursten, L. M.; Danielsen, N. *Biomaterials* **2008**, *29*, 4598–4604.